Mesoporous Materials

Deutsche Ausgabe: DOI: 10.1002/ange.201503295
Internationale Ausgabe: DOI: 10.1002/anie.201503295

Bottom-Up Construction of Mesoporous Nanotubes from 78-Component Self-Assembled Nanobarrels**

*Guang-Lu Zhang, Li-Peng Zhou, Da-Qiang Yuan, and Qing-Fu Sun**

Abstract: *Segmental and continuous hexagonal-packed mesoporous metal–organic nanotubes (MMONTs) with outside diameters of up to 4.5 nm and channel sizes of 2.4 nm were hierarchically constructed by a rational multicomponent self-assembly process involving starting from $[L_2Pd_2(NO_3)_2]$ (L = o-phenanthroline or 2,2′-bipyridine) and 4-pyridinyl-3-pyrazole. An unprecedented crystallization-driven cross-linking between discrete nanobarrel building units by spontaneous loss of the capping ligands to form infinite nanotubes was observed. Such a barrel-to-tube transformation provides new possibilities for the fabrication of MMONTs using the solution bottom-up approach.*

One-dimensional tubular architectures such as carbon nanotubes are of broad interest in many research fields owing to their unique physical and chemical properties.[1] Great efforts have been paid to the efficient synthesis of different tubular materials for application purposes. Artificial nanotubular materials can be categorized into three general types: 1) inorganic nanotubes made of pure carbon,[1a] silicon,[2] metals,[3] or heteroelemental nitrides including BN,[4] AlN,[5] GaN,[6] which have been the research focus of nanomaterials for decades;[7] 2) organic nanotubes formed by end-to-end packing of synthetic macrocycles,[8] peptides,[9] DNA,[10] or other biomolecules;[11] and 3) metal–organic nanotubes (MONTs) constructed from organic ligands (L) and metal ions (M).[12] Owing to their convenient tunability both in composition and topology, MONTs have recently become a topic of vigorous research.[13]

Coordination-driven self-assembly has been proven to be a powerful approach in the bottom-up construction of designable supramolecular architectures.[14] Numerous macrocyclic, polyhedral, and spherical structures have been designed with various types of organic ligands and metal ions based on elaborate symmetry considerations.[14,15] However, the directional self-assembly of infinite 1D mesoporous tubular structures has rarely been explored, though a few examples of discrete open-ended nanotubes have been documented.[16]

The Fujita group has established a family of spherical complexes with empirical formula $\{M_nL_{2n}\}$ that can be self-assembled by simply mixing banana-shaped bidentate pyridine ligands and bare square-planar Pd^{II} ions.[17] Meanwhile, the Yu group has reported that a series of macrocyclic or caged complexes can be synthesized using multidentate pyrazole-based ligands and a dimetallic Pd^{II} clip.[18] In the latter case, the spontaneous deprotonation of the pyrazole ligands during the self-assembly and the saddle-like shape of the resulting structural unit suggest the robustness of these complexes, which could be used as secondary building units (SBUs) in the construction of more sophisticated architectures. Indeed, Yu et al. has previously reported that homo- or heterometallic square complexes can be obtained in a programmable manner by taking advantage of such an SBU.[18e]

With these precedents in mind, we report the rational bottom-up self-assembly of discrete hexagonal nanobarrels **4** formulated as $\{Pd_{30}L^1_{24}L^2_{24}\}$ and consisting of as many as 78 components. Furthermore, we report their crystallization-driven conversion into segmental or continuous mesoporous MONTs (MMONTs) with a large out-diameter of up to 4.5 nm and a channel size of 2.4 nm (Scheme 1).

Ligand **2**, which contains both pyrazole and pyridine moieties, was subjected to stepwise complexation. It first reacted on the pyrazole side with capping dimetallic clip **1** to form SBU **3**, then the pyridine units coordinated to bare Pd^{II} ions to afford larger assemblies.

Complex **3a** was obtained quantitatively by reacting ligand **2** with an equimolar amount of $[(phen)_2Pd_2(NO_3)_2]$ (**1a**; phen = *o*-phenanthroline) in aqueous solution at 100 °C for 5 h. To neutralize the compound for further coordination to other metal centers, **3a** was isolated as its hexafluorophosphate salt by precipitation with excess KPF_6. Its structure was confirmed by NMR and ESI-TOF-MS spectroscopy (See the Supporting Information for details). Then **3a** (PF_6^-salt, 10 μmol) was treated with $Pd(PF_6)_2$ (5 μmol) in $[D_6]$DMSO with continuous stirring at 50 °C for 5 h, which resulted in a clear yellow solution.

As the SBU itself can serve as a 90° curved bidentate ligand, we first envisaged that an M_6L_{12}-type molecular-cube structure would be obtained. To our surprise, the resulting complex was not the cube, but instead hexagonal nanobarrel **4**; this was possibly due to the lack of planarity between the two pyridine rings in the SBU.

The quantitative formation of a giant and highly symmetric product was first suggested by the considerable

[*] G.-L. Zhang, Dr. L.-P. Zhou, Prof. Dr. D.-Q. Yuan, Prof. Dr. Q.-F. Sun
State Key Laboratory of Structural Chemistry
Fujian Institute of Research on the Structure of Matter
Chinese Academy of Sciences, Fuzhou 350002, Fujian (P.R. China)
E-mail: qf-sun@fjirsm.ac.cn
G.-L. Zhang
University of Chinese Academy of Sciences
Beijing 100049 (P.R. China)

[**] This work was supported by the National Natural Science Foundation of China (Grant Nos. 21402201, 21471150) and start-up funding from FJIRSM-CAS. Q.-F.S. acknowledges the award of "The Recruitment Program of Global Youth Experts". Beam time at SSRF is acknowledged (Project no. 14SRBL17U19745).

Supporting information for this article is available on the WWW under http://dx.doi.org/10.1002/anie.201503295.

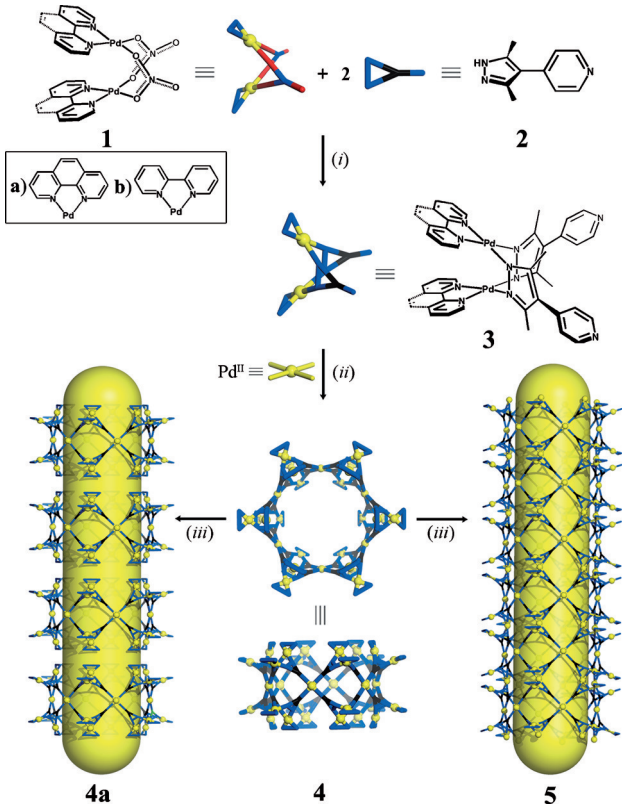

Scheme 1. Representation for the hierarchical self-assembly of segmental (**4a**) and continuous (**5**) MMONTs and starting from dimetallic clips **1** and ligand **2**. Conditions: i) H_2O, 100 °C, 5 h; ii) DMSO, 50 °C, 5 h; iii) crystallization by dioxane diffusion into a DMSO solution of **4**.

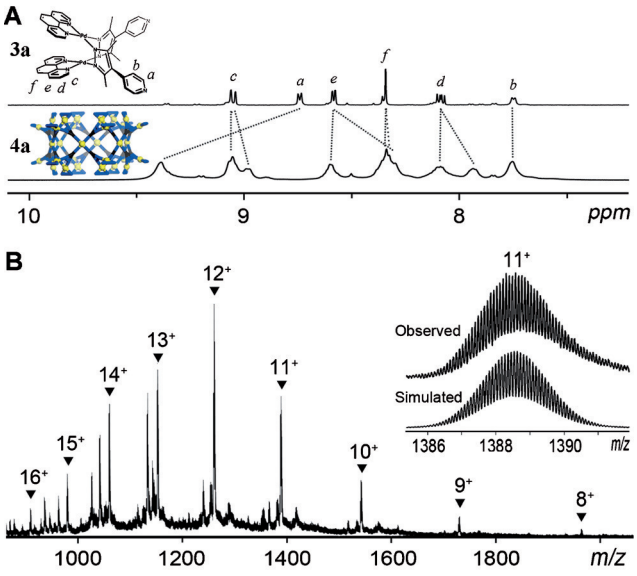

Figure 1. A) ^{1}H NMR spectra (400 MHz, [D$_6$]DMSO, 300 K) of **3a** and **4a** (PF_6^- salt). B) ESI-TOF-MS spectrum of **4a** (PF_6^- salt) with an inset showing the observed and calculated isotope patterns of the 11^+ peak.

broadening and simplicity of the ^{1}H NMR spectrum of **4a** (Figure 1 A). All of the proton signals were fully assigned based on a ^{1}H–^{1}H COSY experiment. The downfield shift of 0.61 ppm for the Py$_\alpha$ signals (H$_a$ in Figure 1 A, Py = pyridine) indicates that a further complexation occurred in the second reaction step. It is noteworthy that the protons of phen (H$_{c,d,e,f}$) on **3a** have split into two sets in a 1:1 ratio; one of these two sets of signals has no obvious chemical shift but the other is clearly upfield-shifted. This suggests that there are two different chemical environments for the phen groups in the final product. The diffusion-ordered spectroscopy (DOSY) NMR spectrum suggests the formation of a single product with a single diffusion coefficient of 6.26×10^{-11} m^{2}s^{-1}, from which a diameter of 3.2 nm was calculated based on the Stokes–Einstein equation (Supporting Information, Figure S15). Dynamic light scattering (DLS) confirmed the monodispersity of the product in solution, with a reported size distribution by volume of 99.9 % at around 3.2 nm (Supporting Information, Figure S24).

The composition of complex **4a** as $\{(phen)_{24}Pd_{30}\mathbf{2}_{24}(PF_6)_{36}\}$ was clearly provided by ESI-TOF-MS measurements. The prominent peaks observed at $m/z = 909.5131$, 979.7468, 1060.0833, 1152.7025, 1261.0115, 1388.5550, 1541.8068, 1729.6691, and 1963.2667 correspond to $[\mathbf{4a}-(PF_6^-)_n]^{n+}$ (n = 16–8). Moreover, the isotopic patterns of each peak were in good agreement with the calculated values, which further confirms the huge molecular weight of 16868.6 Da (Figure 1 B).

The structure of complex **4a** was unambiguously determined by X-ray diffraction analysis. Single crystals suitable for crystallographic analysis were obtained by the slow vapor diffusion of 1,4-dioxane into a DMSO solution of **4a** over two weeks. As a consequence of the huge unit cell and severe disorder of the anions and solvent molecules, the diffraction power of the crystals is limited in nature. Nonetheless, high-quality diffraction data to a resolution of 1.1 Å were obtained on a synchrotron beamline at the Shanghai Synchrotron Radiation Facility (SSRF).

In the crystal structure of **4a**, 12 dimetallic clips are connected by six square-planar coordinated Pd^{II} ions in a cyclic fashion. This forms a giant nanobarrel assembly with an out-diameter of 4.5 nm and a height of 2.6 nm (Figure 2 A,B). To the best of our knowledge, with 78 components, this discrete unique structure contains the largest total number of components reported so far for an organopalladium complex. The two orientations of the phen rings, 12 of which sit on the waist and 12 on the rim of the barrel, account very well for the two sets of ^{1}H NMR signals observed in solution. The dihedral angles between the coordination planes of the phen ligands in the dimetallic clips are close to 90°, which suggests that there are no π–π interactions between them. The separation between the two Pd^{II} ions in the dimetallic clips is 3.24 Å, which indicates the existence of weak Pd^{II}···Pd^{II} interactions. These are commonly observed in self-assemblies using the dimetallic clips. Along the *c* axis, nanobarrels **4a** are packed coaxially in an end-to-end fashion with a separation of 3.9 Å between the closest phen hydrogen atoms. This forms a segmented tubular structure with an infinite 1D mesoporous channel (Figure 2 C). In the *ab* plane, these segmental MMONTs are loosely hexagonally packed with weak π–π stacking interactions between the neighboring phen rings perpendicular to the nanotube surface. This

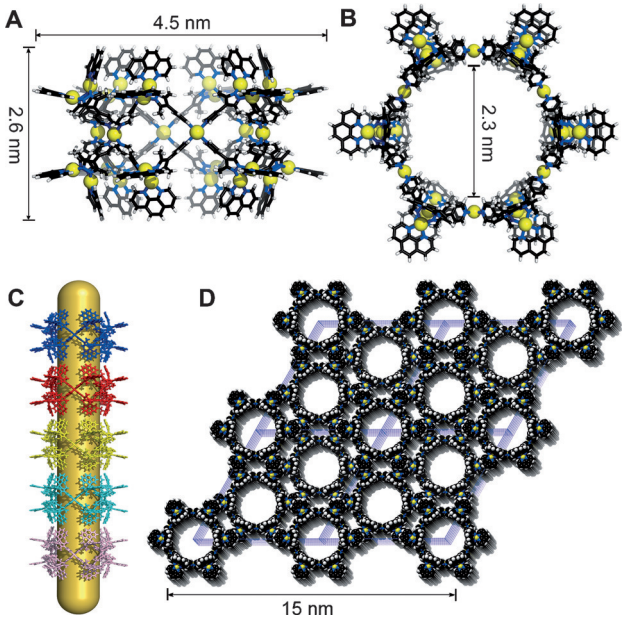

Figure 2. A) and B) Perspective views of the crystal structure of **4a** with dimensions marked in nm. C black, H white, N blue, Pd yellow. Counterions have been omitted for clarity. C) Coaxial packing of nanobarrels (highlighted in different colors for distinction) to form segmental nanotubes with a mesoporous channel. D) Hexagonal packing (2×2×6 unit cells) of the segmental nanotubes viewed along the *c* axis.

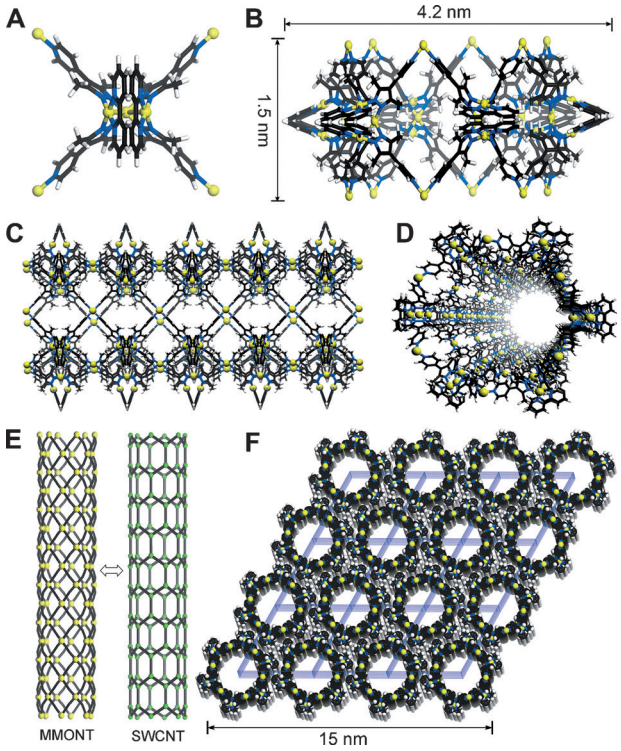

Figure 3. A) Structural unit of the crystal structure of MMONT **5** (note that the two {(bpy)Pd^{II}} capping units each have only 50% occupancy). B) One barrel segment of **5**. C) and D) Perspective views of five segments of nanotube **5**. E) Topological comparison of **5** (MMONT) with a single-walled carbon nanotube (SWCNT) with a (6,0) index. F) Hexagonal packing (3×3×6 unit cells) of **5** viewed along the *c* axis.

packing results in an additional six small channels along the *c* axis (Figure 2D).

When using $[(bpy)_2Pd_2(NO_3)_2]$ (**3b**; bpy = 2,2′-bipyridine) instead of **3a**, ^{1}H NMR, DOSY, ESI-TOF-MS, and DLS spectroscopic data (Supporting Information, Figures S14, 17, 22, 23, 25) all confirmed the quantitative formation of barrel-like discrete complex **4b** in solution. However, it is interesting to note that discrete barrel structure **4b** is transformed into infinite MMONT **5** during the crystallization process (Figure 3). A prism block crystal of **5** was grown by vapor diffusion of 1,4-dioxane into a DMSO solution of **4b**, the same method as used for the crystallization of **4a**. In the crystal structure, the external capping units {(bpy)Pd^{II}} on **4b** are partially dissociated and the nanobarrels are connected to form the continuous tubular structure by further coordination to their neighbors.

Conceptually, the structural unit of **5** can be regarded as a C_{2v} symmetrical cambered building block, consisting of four ligands **2** and a Pd_3 cluster (Figure 3A). It is worth pointing out that only one {(bpy)Pd^{II}} capping unit is found on the top of the Pd_3 cluster, which is disordered over two possible conformations. This suggests the possibility of using the leftover chelation sites around the nanotubes as active sites for heterogeneous catalysis. The pyrazole moieties of **2** are coordinated to the Pd_3 cluster whereas the pyridine arms point outward to link the square-planar Pd^{II} centers. Six such units are bridged together in a cyclic manner to form one barrel segment (Figure 3B), which is then further cross-linked along the *c* axis to form infinite 1D MMONT **5** (Figure 3C,D). Topologically, this tubular structure can be described as a rolled-up cylinder of a (4,4)-square sheet, analogous to the zigzag single-walled carbon nanotube with an index defined as (6,0) (Figure 3E). In the *ab* plane, discrete nanotubes of **5** are bundled together in a hexagonal fashion similar to **4a** (Figure 3F). Denser packing was observed in **5** than in **4a** owing to the smaller size of the capping ligand on the surface (bpy instead of phen).

The observed barrel-to-tube conversion is worthy of further discussion. As **4a** and **4b** differ only in the capping ligands on their surface, we tentatively rationalized this crystallization-driven transformation with their inherent stability differences. First, it is well-known that phen is a stronger ligand than bpy, which helps to hold the multi-component self-assembled complex together in solution. The loss of auxiliary bpy ligands in self-assembled palladium complexes has been documented.[19] In fact, dissociation of the capping {(bpy)Pd^{II}} units was also observed in the ESI-TOF-MS spectra of complex **4b**, but not in the spectra of complex **4a** (Supporting Information, Figure S22). Second, π–π stacking interactions between the phen rings may also provide additional stability in the crystal structure of **4a**, whereas no such interactions were observed in **5**.

Scanning electron microscopy (SEM) showed that tube **5** formed microfibril structures, whereas barrel **4a** had a microspherical mophology (Supporting Information, Figure S26–27). As a proof-of-concept experiment, fine powdered

Table 1: Suzuki–Miyaura coupling reaction between aryl iodide and *p*-tolylboronic acid catalyzed by **4a** or **5**.[a]

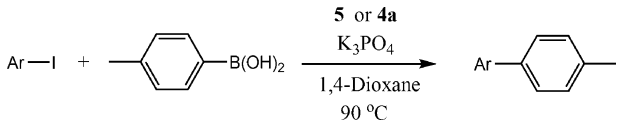

Entry	Ar	Pd [mol%]	Yield [%][b] for **4a**	Yield [%][b] for **5**
1	phenyl	0.45	60	98
2	4-acetylphenyl	0.45	58	99
3	4-fluorophenyl	0.45	59	98
4	4-methoxyphenyl	0.45	56	98
5	2-pyridyl	0.45	43	58

[a] All reactions were performed on a 0.1 mmol scale using 300 mol% K_3PO_4 and 0.015 mol% **4a** or 0.018 mol% **5** (empirical formula weight based on one barrel segment unite of the tube as shown in Figure 3 B) in 1,4-dioxane (5 mL) at 90 °C for 12 h. [b] Yields were determined by 400 MHz ^{1}H NMR spectroscopy with the aid of CH_2Cl_2 as an internal standard.

samples of **5** and **4a** were tested for catalyzing the Suzuki–Miyaura cross-coupling reactions between aryl iodide and aryl boronic acid (Table 1). The reactions were heterogeneous in nature as they were performed in 1,4-dioxane, a solvent from which the crystals of **5** and **4a** were obtained. Substituted aryl iodides were screened which confirmed that both electron-donating and electron-withdrawing groups could be tolerated (entries 1–5). With as low as a 0.45 mol% loading based on Pd, desirable products were obtained in high yields with **5** as the catalyst, whereas only moderate yields were observed using **4a** instead. Besides, preliminary kinetic studies (Supporting Information, Figures S31–33) revealed that the catalysis by **5** was over 10-fold faster than **4a**. This obvious catalytic difference between **4a** and **5** was attributed to the coordination-unsaturated Pd sites on the ends of tubular **5**.

In summary, the construction of unique MMONT structures has been accomplished by a rational coordination-directed bottom-up fabrication process featuring an unprecedented barrel-to-tube conversion. Formation of either segmental or continuous MMONTs can be easily controlled by choosing appropriate starting materials. This study provides a new strategy for the construction of artificial nanotubular materials through a modular self-assembly method. The synthesis of heterometallic nanotubes with adjustable pore sizes using this strategy and the detailed study of their catalytic properties are currently underway.

Experimental Section

Synthesis of **4a** (PF_6^- salt): Ligand **3a** (PF_6^- salt) (24.12 mg, 19.97 μmol) was treated with $Pd(PF_6)_2$ (3.95 mg, 9.96 μmol) in [D_6]DMSO (1.0 mL) at 50 °C for 5 h. ^{1}H NMR spectroscopy confirmed the quantitative formation of **4a**. An excess amount of a mixture of ethyl acetate and diethyl ether (1:1 in volume) was added to the solution of barrel **4a** and the precipitate was collected by centrifugation and dried in vacuo to give **4a** as a white solid (22.46 mg, 1.33 μmol, 80% yield). M.p. > 320 °C (decomposed). ^{1}H NMR (400 MHz, [D_6]DMSO, 300 K) $\delta = 9.38$ (br, 48H), 9.05 (br, 48H), 8.98 (br, 24H), 8.59 (br, 24H), 8.33 (br, 48H), 8.29 (br, 24H), 8.08 (br, 48H), 7.93 (br, 24H), 7.74 (br, 48H), 2.65 ppm (br, 144H).^{13}C NMR (100 MHz, [D_6]DMSO, 300 K) $\delta = 151.26$, 149.89, 147.06, 145.08, 141.28, 130.64, 127.85, 126.66, 126.26, 125.53, 115.78, 13.71 ppm. Diffusion coefficient ([D_6]DMSO, 300 K): $D = 6.29 \times 10^{-11}$ m^{2}s^{-1} (Log $D = -10.25$). ESI-TOF-MS (PF_6^- salt, CH_3CN): The following picked signals are those at the highest intensities. *m/z* Calcd for $[M-9(PF_6^-)]^{9+}$ 1729.3246, found 1729.3325; Calcd for $[M-10(PF_6^-)]^{10+}$ 1541.8957, found 1541.9005; Calcd for $[M-11(PF_6^-)]^{11+}$ 1388.5448, found 1388.5525; Calcd for $[M-12(PF_6^-)]^{12+}$ 1260.7523, found 1260.7610; Calcd for $[M-13(PF_6^-)]^{13+}$ 1152.6202, found 1152.7812; Calcd for $[M-14(PF_6^-)]^{14+}$ 1059.9356, found 1059.9398; Calcd for $[M-15(PF_6^-)]^{15+}$ 976.6089, found 976.6175. IR (KBr) $\tilde{\nu}$ = 3652, 3420, 3092, 1619, 1540, 1430, 1343, 1222, 1029, 840, 716, 557 cm^{-1}.

Synthesis of **4b** (BF_4^- salt): Ligand **3b** (BF_4^- salt) (21.52 mg, 20.60 μmol) was treated with $[Pd(CH_3CN)_4](BF_4)_2$ (4.56 mg, 10.3 μmol) in [D_6]DMSO (1.0 mL) at 50 °C for 5 h. ^{1}H NMR confirmed the quantitative formation of **4b**. An excess amount of a mixture of ethyl acetate and diethyl ether (1:1 in volume) was added to the solution of barrel **4b** and the precipitate was collected by centrifugation and dried in vacuo to give **4b** as a white solid (17.01 mg, 1.42 μmol, 83% yield). M.p. > 320 °C (decomposed). ^{1}H NMR (400 MHz, [D_6]DMSO, 300 K) $\delta = 9.27$ (br, 48H), 8.63 (br, 48H), 8.41 (br, 24H), 8.33 (br,24H), 8.20 (br, 24H), 7.94 (br, 24H), 7.72 (br, 24H), 7.61 (br, 48H), 7.56 (br, 24H), 2.46 ppm (br, 144H). ^{13}C NMR (100 MHz, [D_6]DMSO, 300 K) $\delta = 156.89$, 150.20, 149.48, 144.98, 142.53, 128.19, 125.46, 124.46, 118.23, 115.60, 22.37 ppm. Diffusion coefficient ([D_6]DMSO, 300 K): $D = 6.28 \times 10^{-11}$ m^{2}s^{-1} (Log $D = -10.20$) ESI-TOF-MS (BF_4^- salt, CH_3CN): The following picked signals are those at the highest intensities. *m/z* Calcd for $[M-8(BF_4^-)]^{8+}$ 1687.9987, found 1687.7384; Calcd for $[M-9(BF_4^-)]^{9+}$ 1490.7766, found 1490.7647; Calcd for $[M-10(BF_4^-)]^{10+}$ 1332.9981, found 1332.9780; Calcd for $[M-11(BF_4^-)]^{11+}$ 1203.9978, found 1204.0711; Calcd for $[M-12(BF_4^-)]^{12+}$ 1096.4144, found 1096.4067. IR (KBr) $\tilde{\nu}$ = 3604, 3413, 2904, 1614, 1540, 1503, 1474, 1455, 1428, 1381, 1351, 1221, 1050, 843, 772, 723, 658, 585, 517 cm^{-1}.

Synthesis of **5**: Single crystals of **5** were obtained by the slow vapor diffusion of 1,4-dioxane into a DMSO solution of **4b** (16.6 μmol) over two weeks. The prism yellow crystals was collected by filtration, washed with 1,4-dioxane several times and dried in vacuo to give **5** (115 mg, 10.4 μmol, 50.1% yield based on Pd). Elemental analysis calcd for $C_{300}H_{298}N_{84}B_{24}F_{96}Pd_{24}\cdot(C_4H_8O_2)_6\cdot((CH_3)_2SO)_{10}$: C 37.5, H 3.63, N 10.68%; found C 37.0, H 3.71, N 10.58%. IR (KBr) $\tilde{\nu}$ = 3445, 2920, 2851, 1751, 1611, 1535, 1457, 1424, 1381, 1311, 1255, 1083, 1027,875, 762, 723, 646, 517 cm^{-1}.

Crystal data for **4a**: Space group $R\bar{3}/m$, $a = b = 66.460(9)$ Å, $c = 30.056(6)$ Å, $V = 114970(45)$ Å^3, $Z = 3$, $T = 293$ K. Anisotropic least-squares refinement for the framework atoms and isotropic refinement for the other atoms on 10274 independent merged reflections ($R_{int} = 0.042$) converged at residual $wR_2 = 0.2708$ for all data; residual $R_1 = 0.0781$ for 19780 observed data [$I > 2\sigma(I)$], and goodness of fit (GOF) = 1.264.

Crystal data for **5**: Space group $P6/m$, $a = b = 39.2398(10)$ Å, $c = 14.9993(5)$ Å, $V = 20001.2(14)$ Å^3, $Z = 6$, $T = 293$ K. Anisotropic least-squares refinement for the framework atoms and isotropic refinement for the other atoms on 13794 independent merged reflections ($R_{int} = 0.0613$) converged at residual $wR_2 = 0.4451$ for all data; residual $R_1 = 0.1477$ for 46043 observed data [$I > 2\sigma(I)$], and goodness of fit (GOF) = 1.157.

Full experimental details and crystallographic analysis are given in the Supporting Information. CCDC 1041046 and 1041047 contain the supplementary crystallographic data for this paper. These data can be obtained free of charge from The Cambridge Crystallographic Data Centre.

Keywords: crystallization-driven cross-linking · mesoporous materials · metal–organic nanotubes · palladium · self-assembly

How to cite: *Angew. Chem. Int. Ed.* **2015**, *54*, 9844 – 9848
Angew. Chem. **2015**, *127*, 9982 – 9986

[1] a) S. Iijima, *Nature* **1991**, *354*, 56 – 58; b) V. Sgobba, D. M. Guldi, *Chem. Soc. Rev.* **2009**, *38*, 165 – 184.
[2] a) D. D. D. Ma, C. S. Lee, F. C. K. Au, S. Y. Tong, S. T. Lee, *Science* **2003**, *299*, 1874 – 1877; b) J. Bai, X. C. Zeng, H. Tanaka, J. Y. Zeng, *Proc. Natl. Acad. Sci. USA* **2004**, *101*, 2664 – 2668.
[3] Y. Sun, Y. Xia, *Adv. Mater.* **2004**, *16*, 264 – 268.
[4] N. G. Chopra, R. J. Luyken, K. Cherrey, V. H. Crespi, M. L. Cohen, S. G. Louie, A. Zettl, *Science* **1995**, *269*, 966 – 967.
[5] L.-W. Yin, Y. Bando, Y.-C. Zhu, M.-S. Li, C.-C. Tang, D. Golberg, *Adv. Mater.* **2005**, *17*, 213 – 217.
[6] a) J. Goldberger, R. He, Y. Zhang, S. Lee, H. Yan, H.-J. Choi, P. Yang, *Nature* **2003**, *422*, 599 – 602; b) M. A. Reshchikov, H. Morkoc, *J. Appl. Phys.* **2005**, *97*, 061301 – 061395.
[7] a) Y. Xiong, B. T. Mayers, Y. Xia, *Chem. Commun.* **2005**, 5013 – 5022; b) J. Goldberger, R. Fan, P. Yang, *Acc. Chem. Res.* **2006**, *39*, 239 – 248.
[8] a) V. G. Organo, A. V. Leontiev, V. Sgarlata, H. V. R. Dias, D. M. Rudkevich, *Angew. Chem. Int. Ed.* **2005**, *44*, 3043 – 3047; *Angew. Chem.* **2005**, *117*, 3103 – 3107; b) G. D. Pantoş, P. Pengo, J. K. M. Sanders, *Angew. Chem. Int. Ed.* **2007**, *46*, 2238 – 2240; *Angew. Chem.* **2007**, *119*, 2288 – 2290; c) T. Iwanaga, R. Nakamoto, M. Yasutake, H. Takemura, K. Sako, T. Shinmyozu, *Angew. Chem. Int. Ed.* **2006**, *45*, 3643 – 3647; *Angew. Chem.* **2006**, *118*, 3725 – 3729.
[9] a) M. R. Ghadiri, J. R. Granja, R. A. Milligan, D. E. McRee, N. Khazanovich, *Nature* **1993**, *366*, 324 – 327; b) T. D. Clark, J. M. Buriak, K. Kobayashi, M. P. Isler, D. E. McRee, M. R. Ghadiri, *J. Am. Chem. Soc.* **1998**, *120*, 8949 – 8962; c) M. Amorín, L. Castedo, J. R. Granja, *J. Am. Chem. Soc.* **2003**, *125*, 2844 – 2845; d) W. S. Horne, C. D. Stout, M. R. Ghadiri, *J. Am. Chem. Soc.* **2003**, *125*, 9372 – 9376.
[10] a) P. Yin, R. F. Hariadi, S. Sahu, H. M. T. Choi, S. H. Park, T. H. LaBean, J. H. Reif, *Science* **2008**, *321*, 824 – 826; b) S. M. Douglas, H. Dietz, T. Liedl, B. Hogberg, F. Graf, W. M. Shih, *Nature* **2009**, *459*, 414 – 418.
[11] a) N. P. King, W. Sheffler, M. R. Sawaya, B. S. Vollmar, J. P. Sumida, I. Andre, T. Gonen, T. O. Yeates, D. Baker, *Science* **2012**, *336*, 1171 – 1174; b) T. Sendai, S. Biswas, T. Aida, *J. Am. Chem. Soc.* **2013**, *135*, 11509 – 11512; c) C. Hou, Q. Luo, J. Liu, L. Miao, C. Zhang, Y. Gao, X. Zhang, J. Xu, Z. Dong, J. Liu, *ACS Nano* **2012**, *6*, 8692 – 8701.
[12] a) R. Kaminker, R. Popovitz-Biro, M. E. van der Boom, *Angew. Chem. Int. Ed.* **2011**, *50*, 3224 – 3226; *Angew. Chem.* **2011**, *123*, 3282 – 3284; b) F. Dai, H. He, D. Sun, *J. Am. Chem. Soc.* **2008**, *130*, 14064 – 14065; c) K. Otsubo, Y. Wakabayashi, J. Ohara, S. Yamamoto, H. Matsuzaki, H. Okamoto, K. Nitta, T. Uruga, H. Kitagawa, *Nat. Mater.* **2011**, *10*, 291 – 295; d) G. Wu, J. Bai, Y. Jiang, G. Li, J. Huang, Y. Li, C. E. Anson, A. K. Powell, S. Qiu, *J. Am. Chem. Soc.* **2013**, *135*, 18276 – 18279; e) T.-T. Luo, H.-C. Wu, Y.-C. Jao, S.-M. Huang, T.-W. Tseng, Y.-S. Wen, G.-H. Lee, S.-M. Peng, K.-L. Lu, *Angew. Chem. Int. Ed.* **2009**, *48*, 9461 – 9464; *Angew. Chem.* **2009**, *121*, 9625 – 9628.
[13] a) P. Thanasekaran, T.-T. Luo, C.-H. Lee, K.-L. Lu, *J. Mater. Chem.* **2011**, *21*, 13140 – 13149; b) A. Ienco, M. Caporali, F. Costantino, A. Guerri, G. Manca, S. Moneti, M. Peruzzini, *J. Coord. Chem.* **2014**, *67*, 3863 – 3872; c) C. R. Murdock, D. M. Jenkins, *J. Am. Chem. Soc.* **2014**, *136*, 10983 – 10988.
[14] a) P. J. Stang, B. Olenyuk, *Acc. Chem. Res.* **1997**, *30*, 502 – 518; b) M. Fujita, *Chem. Soc. Rev.* **1998**, *27*, 417 – 425; c) D. L. Caulder, K. N. Raymond, *Acc. Chem. Res.* **1999**, *32*, 975 – 982.
[15] a) M. M. Conn, J. Rebek, *Chem. Rev.* **1997**, *97*, 1647 – 1668; b) M. Fujita, M. Tominaga, A. Hori, B. Therrien, *Acc. Chem. Res.* **2005**, *38*, 369 – 378; c) R. Chakrabarty, P. S. Mukherjee, P. J. Stang, *Chem. Rev.* **2011**, *111*, 6810 – 6918.
[16] a) T. Yamaguchi, S. Tashiro, M. Tominaga, M. Kawano, T. Ozeki, M. Fujita, *J. Am. Chem. Soc.* **2004**, *126*, 10818 – 10819; b) S. Tashiro, M. Tominaga, T. Kusukawa, M. Kawano, S. Sakamoto, K. Yamaguchi, M. Fujita, *Angew. Chem. Int. Ed.* **2003**, *42*, 3267 – 3270; *Angew. Chem.* **2003**, *115*, 3389 – 3392; c) D. Ajami, J. Rebek, *J. Am. Chem. Soc.* **2006**, *128*, 5314 – 5315; d) C.-Y. Su, M. D. Smith, H.-C. zur Loye, *Angew. Chem. Int. Ed.* **2003**, *42*, 4085 – 4089; *Angew. Chem.* **2003**, *115*, 4219 – 4223.
[17] a) M. Tominaga, K. Suzuki, M. Kawano, T. Kusukawa, T. Ozeki, S. Sakamoto, K. Yamaguchi, M. Fujita, *Angew. Chem. Int. Ed.* **2004**, *43*, 5621 – 5625; *Angew. Chem.* **2004**, *116*, 5739 – 5743; b) K. Suzuki, M. Kawano, M. Fujita, *Angew. Chem. Int. Ed.* **2007**, *46*, 2819 – 2822; *Angew. Chem.* **2007**, *119*, 2877 – 2880; c) K. Suzuki, M. Tominaga, M. Kawano, M. Fujita, *Chem. Commun.* **2009**, 1638 – 1640; d) Q.-F. Sun, J. Iwasa, D. Ogawa, Y. Ishido, S. Sato, T. Ozeki, Y. Sei, K. Yamaguchi, M. Fujita, *Science* **2010**, *328*, 1144 – 1147; e) K. Harris, D. Fujita, M. Fujita, *Chem. Commun.* **2013**, *49*, 6703 – 6712; f) D. Fujita, H. Yokoyama, Y. Ueda, S. Sato, M. Fujita, *Angew. Chem. Int. Ed.* **2015**, *54*, 155 – 158; *Angew. Chem.* **2015**, *127*, 157 – 160; g) Q.-F. Sun, S. Sato, M. Fujita, *Angew. Chem. Int. Ed.* **2014**, *53*, 13510 – 13513; *Angew. Chem.* **2014**, *126*, 13728 – 13731.
[18] a) S.-Y. Yu, M. Fujita, K. Yamaguchi, *J. Chem. Soc. Dalton Trans.* **2001**, 3415 – 3416; b) S.-Y. Yu, H.-P. Huang, S.-H. Li, Q. Jiao, Y.-Z. Li, B. Wu, Y. Sei, K. Yamaguchi, Y.-J. Pan, H.-W. Ma, *Inorg. Chem.* **2005**, *44*, 9471 – 9488; c) S.-Y. Yu, Q. Jiao, S.-H. Li, H.-P. Huang, Y.-Z. Li, Y.-J. Pan, Y. Sei, K. Yamaguchi, *Org. Lett.* **2007**, *9*, 1379 – 1382; d) Q.-F. Sun, K. M.-C. Wong, L.-X. Liu, H.-P. Huang, S.-Y. Yu, V. W.-W. Yam, Y.-Z. Li, Y.-J. Pan, K.-C. Yu, *Inorg. Chem.* **2008**, *47*, 2142 – 2154; e) J. Tong, S.-Y. Yu, H. Li, *Chem. Commun.* **2012**, *48*, 5343 – 5345.
[19] H. S. Sahoo, D. K. Chand, N. B. Debata, *Inorg. Chim. Acta* **2007**, *360*, 31 – 38.

Received: April 11, 2015
Revised: June 10, 2015
Published online: June 30, 2015

